The effect of successful trabeculectomy on the ocular surface and tear proteomics : a prospective cohort study with 1-year follow-up

Anu Vaajanen[1], Janika Nättinen[2], Ulla Aapola[2], Fabian Gielen[1] and Hannu Uusitalo[1,2]

[1] Tays Eye Centre, Tampere University Hospital, Finland

[2] SILK, Department of Ophthalmology, Faculty of Medicine and Health Technology,

Tampere University, Finland

Corresponding author: Anu Vaajanen, MD, PhD, FEBO

Address: Tays Eye Centre, Tampere University Hospital, Biokatu 14, 33520 Tampere,

Finland

Email: anu.vaajanen@fimnet.fi

Phone: +358-3-31164852

Fax: +358-331164365

Abstract

Purpose: To report changes in the ocular surface and tear proteomics after discontinuation of chronic glaucoma medication.

Methods: Patients requiring trabeculectomy were recruited from the glaucoma clinic of Tampere University Hospital, Finland. Fifty-seven patients with previous history of anti-glaucomatous eye drops (8.1±6.8 years) and having undergone a successful trabeculectomy were included in this report. Outcomes of interest were conjunctival redness grading, tear secretion (Schirmer I) and tear film proteomics (SWATH-MS) in addition to thorough clinical examination. The protocol included five time points: preoperative visit and postoperative visits at month 1, 3, 6 and 12. All parameters measured were compared to the corresponding preoperative levels of each individual eye.

Results: Conjunctival redness and irritation were significantly reduced during follow-up, while tear production remained unchanged. Protein profiles of the tear film indicated significant changes in the ocular surface. Lipid transport was increased while several proinflammatory proteins were consistently decreased after the surgery.

Conclusion: Clinical signs as well as the proteomics results indicated that the trabeculectomy and resulting cessation of topical glaucoma medication were very beneficial to the ocular surface. The state of the conjunctiva improved throughout the 1-year follow-up while the levels of pro-inflammatory proteins decreased and lipid transport-associated functions were increased.

Key words: glaucoma, medication, surgery, tear proteomics

Introduction

Glaucoma is a chronic optic neuropathy with a multifactorial etiology and it is the leading cause of irreversible blindness worldwide (Flaxman et al. 2017). The disease usually progresses slowly and is thus symptomless for the patient, but if left untreated, it can lead to permanent visual field defects and even to blindness. According to contemporary knowledge, the only way to slow down the course of glaucoma is a reduction of intraocular pressure (IOP), which can be achieved with topical glaucoma drugs, laser and surgery. The majority of early glaucoma cases are still treated with topical drugs, although other options such as chamber angle laser and MIGS (minimal invasive glaucoma surgery) are becoming more common (Gazzard et al. 2019, Lee et al. 2019, Shah 2019). Long-lasting topical medications may have several adverse effects, e.g. irritation, redness and chronic inflammation due to toxic or allergic reactions of the ocular surface, which in turn may compromise the potency of drugs and reduce the treatment compliance of patients (Nordmann et al. 2003, Leung et al. 2002). Side effects are often connected to the nature of the preservative included in the medication (Uusitalo et al. 2010, Zhang 2019, Helin-Toiviainen 2015). Surgical treatments are indicated when glaucoma defects progress due to inadequate control of IOP or allergic/toxic reactions against the drugs. Roughly three per cent of Finnish glaucoma patients proceed to filtration surgery such as trabeculectomy, deep sclerectomy or tubes (Parkkari et al. 2019, Glaucoma: Current Care Guidelines, 2014). However, the real number of glaucoma surgeries performed worldwide is not known (Mansouri et al. 2013).

The objective of this paper is to describe the clinical and biological changes taking place on the surface of the eye when the chronic glaucoma medication is discontinued after a successful trabeculectomy.

Materials and methods

Study population:

The study was conducted in accordance with the International Conference of Harmonization Good Clinical Practice guidelines and the Declaration of Helsinki. It was approved by the Ethics Committee at Tampere University Hospital (ETL no R13166). The patients (n=57) were collected from a glaucoma clinic Department of Ophthalmology, Tampere University Hospital, Finland. The inclusion criteria were that the patient had to be over 18 years old and have a glaucoma with a need of filtration surgery. Patients with previous ocular surgeries less than one year before the trabeculectomy were excluded. The need for each operation was determined by a glaucoma specialist. Each patient gave a written informed consent before inclusion in the study. The patients in this analysis had undergone a complete and successful trabeculectomy without any additive anti-glaucomatous medication or glaucoma surgical manipulation during the 1-year follow-up.

Study outline:

Clinical examinations, including ocular surface imaging and Schirmer I test, were performed at 1 month preoperatively and at 1, 3, 6 and 12 months postoperatively. Medical information of the patients' age, sex, diagnosis, current topical treatment and its duration and previous surgeries and treatments were recorded only at the preoperative visit. See Fig. 1 for visualized study protocol details.

Parameters of interest were:

1) Visual acuity measured by automated refractometry (Nidek®, Nidek Co Ltd, Gamagori, Japan)

2) Intraocular pressure measured by a rebound tonometer (Icare Tonometer®, Icare Finland Oy, Vantaa, Finland)

3) Visual fields by static perimetry (SitaFast Program by Visual Field Analyzer, Humphrey Perimetry®,Carl Zeiss Meditec Ab, Jena, Germany)

4) Thickness of cornea measured by ultrasound pachymeter (Pachmate 2®, DGH Technology, Inc., Exton, PA, USA).

5) Tear production measured by Schirmer's I test (Tear Touch, Madhu Instruments, New Delhi, India)

6) Conjunctival grading. Evaluation was made by two independent observers comparing conjunctival state in vivo (unblinded) with a grading photographs (SILK-HU conjunctival scale) and afterwards by comparing conjunctival images taken with the same grading photographs (blinded). The conjunctival reaction was reported between scores 0 to 4. Zero meaning a peaceful conjunctiva and 4 a very irritated conjunctiva.

7) Proteomics of the tear fluid. Schirmer strip samples from 33 patients were analyzed by mass spectrometry (AB Sciex, Concord, Canada).

Surgical procedure:

Three days prior to trabeculectomy, topical dexamethasone-chloramphenicol (Oftan Dexa-Chlora®, Santen Oy, Tampere, Finland) eye drop use (one drop for each eye, 4 times per day) was initiated and this treatment continued 4 weeks after the surgery. After the four-week postoperative follow-up visit, only dexamethasone (Oftan Dexa®, Santen Oy) was used, gradually tapering the dosing, until the treatment stopped at 12 weeks after the

operation. All anti-glaucoma medication, including oral acetazolamide, was discontinued at the time of the operation (See Fig. 1 for a study outline giving pre- and postoperative medication duration). Trabeculectomy was performed under topical anesthesia by oxybuprocain (Oftan Obucain®, Santen Oy) by one surgeon (A.V.). Prior to surgery, 1 gtt pilocarpine 4 mg/ml (IsoptoCarpine ®, Novartis Finland Oy, Espoo, Finland) and 1 gtt apraclonidine 10 mg/ml® (Iopidine®, Novartis Finland Oy) were instilled in the eye. A corneal traction suture (8/0 silk) was used in order to rotate the eyeball to guarantee the operator a good view. Conjunctiva and tenon were opened superiorly in fornix-based manner. Gentle diathermy was performed and a 3x4 mm scleral flap prepared. Swabs moistened with 0.2 mg/ml mitomycin C were used for 2 minutes in the sub-Tenon's space, and immediately after their removal the surface of eyeball was carefully rinsed with balanced salt solution. The anterior chamber was slightly filled with viscoelastic substance (Viscoat®, Alcon, Fort Worth, MD TX, USA) through a small paracentesis. Trabeculectomy was performed using a Khaw punch of 0.5 mm (Duckworth and Kent, Hertfordshire, UK), followed by iridectomy. The flap was closed with 2-5 sutures (10/0 nylon). The amount of flap sutures depended on the preoperative pressure and target pressure levels (postoperative laser suturolysis was performed within two weeks if needed, altogether for 10 out of 57 patients). Both conjunctiva and tenon were closed watertight with 10/0 nylon. At the end of the operation 100 µl bevacizumab 25 mg/ml (Avastin®, Roche Oy, Espoo, Finland) was injected into the anterior chamber, where it spread into sub-Tenon's space. In addition, 0.5 ml dexamethasone sodium phosphate 5 mg/ml (Oradexon ®, Aspen Nordic, Ballerup, Denmark) was injected subconjunctivally into the inferior fornix.

Tear collection and sample preparation:

Tear fluid samples were collected preoperatively and 1, 3, 6 and 12 months after the surgery from closed eyes using Schirmer strips (Tear Touch, Madhu Instruments, New Delhi) without anesthesia. In each visit, the strips were placed under the lower eyelid for 5 minutes and after removal, the strips were stored in -80°C to await further processing. More in-depth description of the sample preparation steps is described in our previously published paper (Nättinen et al. 2018).

In brief, tear samples were solubilized with 0,5% SDS and protein concentration was measured with DC protein assay kit (Bio-Rad laboratories Inc, Hercules, USA). Next, acetone-precipitated proteins were re-solubilized with 2% SDS, reduced with tris-(2-carboxyethyl)phosphine (TCEP) and alkylated with iodoacetamide (IAA) on 30 kDa molecular weight cut-off filters (Pall Corporation, Port Washington, NY, USA). Samples were digested with TPCK-treated trypsin (Sciex, Framingham, USA) at an enzyme-to-protein ratio of 1:25 and cleaned and desalted with C18 tips (Thermo Fisher Scientific) prior to LC-MS analysis. All reagents were purchased from Sigma-Aldrich (St. Louis, MO, USA) unless otherwise stated.

Protein identification and quantification with SWATH-MS:

Digested tear peptides were analysed with Eksigent 425 NanoLC coupled to high-speed TripleTOF™ 5600+ mass spectometer (AB Sciex, Concord, Canada).   First, tear peptides were loaded onto a trap column (120 Å, 200 µm × 0.5 mm) and separated using a nano cHiPLC column (120 Å, 75 µm × 15 cm). Then the peptide mix was introduced into the mass spectrometer (MS) via nanospray source and analysed with 120 min 6 step gradients using eluent A (0.1% FA in 1% ACN) and eluent B (0.1% FA in ACN) at 300 nl/min. The same amount of protein was always loaded to MS analysis. The key

parameters used in the mass spectrometry analysis and additional information of the NanoLC and MSTOF methodology have been extensively described in our previous papers (Nättinen et al. 2018; Jylhä et al. 2018, Nättinen et al. 2020).

A tear fluid spectral library was created by data-dependent acquisition (DDA) method using Protein Pilot® 4.5 (Sciex, Redwood City, USA) using false discovery rate (FDR) of 1% and the DDA runs' MS/MS spectra were identified against UniProtKB/Swiss-Prot human database. The more specific analysis parameters implemented to the ProteinPilot can be found from our previous article (Nättinen et al. 2018). Protein quantification against the obtained spectral library was performed using PeakView® and MarkerView® software (Sciex, Redwood City, USA). Retention time calibration was implemented for all samples using up to three proteins and 1-15 peptides for peak area calculations. Protein quantification results are presented as a combination of protein specific peptides peak intensities from SWATH-MS measurement and here referred to as protein expression.

Statistical analysis:

The postoperative values of clinical variables were compared to the patients' corresponding preoperative values, which were measured when anti-glaucoma medication was still maintained. Clinical changes after trabeculectomy were evaluated with two-tailed paired t-test or Wilcoxon signed rank test for continuous and ordinal variables, respectively. Mean, median and 95% confidence interval (CI) values were calculated for the clinical variables at the preoperative visit as well as postoperative visits 1, 3, 6 and 12 months after the surgery.

For tear fluid proteomics, smaller subset of patients was used (33 out of 57). Schirmer strip tear samples in all five time points were analyzed with mass spectrometry. The

quantitative proteomics data was first transformed to $\log_2$ scale and normalized using central tendency normalization. Permuted correlation-associated p-values were calculated for samples including at least two replicate MS runs, in order to evaluate the quality of the runs. After all initial clean-up and normalization, the replicate MS runs were combined by calculating mean for each protein resulting in one protein expression value per sample. Differential expression analysis evaluating the postoperative changes in tear fluid was performed using Wilcoxon signed rank test assuming dependence between the repeated measures. Due to multiple comparisons, the p-values obtained from the differential expression analysis were adjusted with Benjamini-Hochberg procedure. P-value (adjusted) below 0.05 was used as the statistical significance threshold, unless stated otherwise. Online database tool STRING (Szklarczyk et al. 2019) was used to identify protein-protein interaction networks and QIAGEN's IPA (QIAGEN Redwood City, USA) was used to identify the common biological functions and upstream regulators affected by the surgery and cessation of topical glaucoma medication. All other statistical analyses were performed using R software version 3.5.3 (R Core Team, Vienna, Austria).

Results

The complete clinical data including 57 patients consisted of 46 females (81%) and 11 males (19%), and the mean age was 69.6±7.9 years (range: 49-84 years). Thirty (53%) patients were diagnosed with primary open-angle glaucoma, while 14 (25%) patients had normal-tension glaucoma, 9 (16%) had capsular glaucoma, 3 (5%) had chronic angle-closure glaucoma and 1 (2%) patient had secondary glaucoma. The patients had received medication for their glaucoma for 8.1±6.8 years (range: 1-25 years) and the most recent glaucoma medication had been in use for 1.9±1.8 years (range: 0-8 years). Prior to surgical treatment, the patients had used on average 2.1±0.9 (range 0-5) glaucoma

medications simultaneously. Of the 57 patients included in the study, 18 patients were only on preservative-free glaucoma medication while 39 patients had at least one antiglaucomatous drug with preservatives.   The preoperative visual acuity was 0.1±0.2 in logMAR scale (range: -0.1-1), corresponding to 0.8 in the decimal visual acuity scale, and IOP was 17.9±8.4 mmHg. In visual fields, mean deviation (MD) value was -9.9±6.3 dB (range: -26.4-1.3) and Visual Field Index (VFI) was 71.9±19.7%. The average thickness of cornea was 510.6±31.3 µm and Schirmer's test was on average 14.8±10.3 mm before surgery. The initial conjunctival grading scores (both blinded and unblinded) indicated conjunctival irritation with means of 2.7±0.7 and 2.1±1.0, respectively.

As shown in Table 1 and Fig. 2, conjunctival grading scores as well as IOP values reduced significantly after the surgery throughout the follow-up time. This effect was seen already at the 1-month follow-up and was continued until the 1-year follow-up visit. Other measured clinical variables i.e. mean visual acuity, Schirmer's test, MD and VFI, remained constant during the 1-year follow-up. One eye needed cataract extraction 11 months after trabeculectomy.

Proteomics analyses were performed with 33 out of the 57 patients, equaling to 165 processed Schirmer strip tear samples. The clinical results for the subgroup of 33 patients were very similar to the findings with the complete patient data (Supplementary Table S1). The Schirmer strip samples from 33 patients produced a tear proteomics dataset with 868 proteins, of which 217 proteins were significantly changed 1 year after the surgery (adjusted p-value < 0.05) (Supplementary Table S2). Altogether 65 proteins had altered expression level after the surgery in at least 3 time point comparisons; 48 proteins had decreased and 17 had increased expression levels after the surgery (Supplementary Table S3). Twelve proteins of interest have been further visualized in Fig. 3, including apolipoproteins E and M (APOE and APOM), mucin-like protein 1 (MUCL1) and vacuolar

protein sorting-associated protein 4A (VPS4A) with increased postoperative expression levels and calmodulin (CALM1), alpha-enolase (ENO1), glutathione peroxidase 3 (GPX3), glutaredoxin-1 (GLRX), neutrophil gelatinase-associated lipocalin (LCN2), prolactin-inducible protein (PIP), proteasome subunit alpha type-6 (PSMA6), S100 proteins (S100A11, S100A4, S100A8 and S100A9) and superoxide dismutase [Mn] (SOD2) with decreased expression levels. According to STRING database, the 48 decreased proteins were connected to cell secretion, glucose metabolic process and oxidation reduction process, while the 17 increased proteins were associated with lipid and cholesterol transport and cellular component organization (Fig. 4 and Table 2). Both increased and decreased proteins were related to immune effector process.

We also examined the biological functions associated with individual time points in order to identify, whether any functions changed direction during time or took place only in specific time points. As illustrated in Fig. 5, cell movement of immune cells and inflammatory responses were decreased, and cell death was increased especially in the early time points. Lipid metabolism and free radical scavenging were increased 1 year after the surgery. IPA also identified some upstream regulators driving the protein changes; e.g., several cytokines, including IFNG, TNF, IL1B and IL6, appeared to have significantly decreased expression in majority of postoperative time points. Further details can be found from Supplementary Table S4.

Discussion

Trabeculectomy was developed in the 1960's (Cairns et al. 1968) and has since become the "gold standard" of glaucoma surgery, as it is proven to be one of the most efficacious therapeutic choices in glaucoma care (Migdal et al. 1994). In most cases, the patients do

not require additional topical glaucoma medication for years or even decades (Landers et al. 2012). The main risk factors for failure of glaucoma surgery are chronic irritation and inflammation of the conjunctiva, which are closely connected to the wound healing process that in excess will seal the newly formed outflow channels (Skuta & Parrish 1987, Broadway et al. 1994, Helin et al. 2011).

According to our results, the health status of the ocular surface improved significantly after successful trabeculectomy and cessation of topical glaucoma medication during the 1-year follow-up. The clinical signs of ocular surface irritation, evaluated with a 0-4 grading system during the visit (unblinded) as well as from photographs (blinded), were already significantly decreased one month after the operation and the grades remained at lower levels throughout the follow-up period. This is most likely due to the withdrawal from the glaucoma medication as well as anti-inflammatory, e.g. glucocorticoid, therapy during and after the operation. According to previous studies, the inflammatory signs in conjunctiva decrease relatively slowly after withdrawal of preservatives (Uusitalo et al. 2010, Uusitalo et al. 2016, Nättinen et al. 2018), and therefore, it is probable that the rapid attenuation of the inflammatory signs during the first postoperative months in our study is mainly due to the efficacious anti-inflammatory therapy. After the gradual tapering of the topical glucocorticoid dosing after the 1-month follow-up visit, we are able to observe the slower effects taking place after the cessation of glaucoma medication.

Pre-, peri- and postoperative anti-inflammatory treatment is a vital part of modern glaucoma surgery and mainly used to prevent the excess of wound healing, scar formation and thus surgical failure (Breuseqem et al. 2009, Almatholouh et al. 2018). In our study, topical glucocorticoids, which are highly effective anti-inflammatory compounds, were used topically before the surgery, as a perioperative subconjunctival injection and the treatment was continued for three months following the operation. Our protocol also included the use

of intraoperative mitomycin C under the conjunctiva and tenon capsule as well as intracameral bevacizumab, which also affect the inflammation and wound healing responses (Wilkins et al. 2005, Li et al. 2009, Vandewalle et al. 2014). The effects of these anti-inflammatory therapeutic interventions in our protocol are estimated not to exceed 3 months. Therefore, the improvements seen in clinical signs beyond this time point are expected to be connected to the withdrawal from glaucoma medication.

Clinical improvement of the ocular surface after trabeculectomy and withdrawal from glaucoma medication was also reflected to the tear fluid protein profiles. The proteins, which were consistently decreased after the surgery included various proinflammatory proteins, such as S100A proteins (S100A4, S100A8, S100A9 and S100A11), CALM1 and ENO1, but also other well-known tear fluid proteins including PIP and IGHG1. The S100A proteins and ENO1 are often found increased in dry eye and at least CALM1, IGHG1, S100A8 and S100A9 have been observed to be increased due to glaucoma and prolonged glaucoma medication in particular (Zhou et al. 2009, Perumal et al. 2016, Wong et al. 2011, Pieragostino et al. 2012). Thus, a decrease in these proteins' expression levels suggests favourable changes in the ocular surface. The article by Wong et al. also reported that glaucoma medication induced an increase of 14-3-3 protein zeta/delta (YWHAZ) and mammaglobin B (SCGB2A2) and a decrease of proline-rich 4 protein (PRR4). Although according to our results only YWHAZ had a statistically significant decrease 1 year after the trabeculectomy, overall the fold changes indicated a decrease of YWHAZ and SCGB2A2 and an increase of PRR4 (not shown), again suggesting an improvement in the state of the ocular surface. PIP, which was also decreased after the surgery, has previously been observed to be decreased in primary open angle and pseudoexfoliative glaucoma, possibly indicating the disease progression (Pieragostino et al. 2012). Overall, the observed reduction of proinflammatory proteins does support to

some degree the decrease of immune response and immune cell migration, however, according to our results these biological functions are mainly taking place on the early stages, i.e. 1 or 3 months after the surgery, while the proinflammatory proteins identified in our study decreased consistently throughout the follow-up period. Hence, as discussed in relation to the improved conjunctival state, the proinflammatory proteins' reduction could be connected to the favorable decreases in IOP and cessation of topical glaucoma medication, while immune response suppression could be originating from the perioperative medications necessary for a successful trabeculectomy.

In addition to increased levels of proinflammatory proteins, the pathway and functional enrichment analyses suggested that the generation of reactive oxygen species (ROS) were notably increased in comparison to the baseline at the 1-year time point, while various metabolic functions were downregulated, including oxidation-reduction process. Previously, ocular inflammatory diseases have been associated with the generation of ROS (Dogru et al. 2018) and for example superoxide dismutase (SOD) and proteins from the glutathione peroxidase (GPX) family have been known to participate in the inhibition of ROS (reviewed by Ighodaro & Akinloye 2018). From the visualizations in Fig. 3, decreased levels of antioxidants GPX3 and SOD2, which protect the cells from oxidative stress could be seen and other SOD isoenzymes (SOD1 and SOD3) had also decreased expression levels in our data, although the differences were not statistically significant. A previous study by Ferreira et al. (2004) found a significantly increased expression levels of superoxide dismutase (SOD) in glaucoma patients' aqueous humor, which indicated an increased oxidative stress condition in the eye. GLRX and LCN2 have similarly been identified as antioxidants reducing ROS and oxidative stress and found upregulated under harmful conditions, suppressing inflammation (Sun et al. 2017, Liu et al. 2015, Roudkenar et al. 2007, Tang et al. 2018). The reduction of the aforementioned antioxidants could

therefore indicate that the levels of ROS and oxidative stress have decreased in tear fluid due to improved ocular surface condition, given that the balance between pro- and antioxidant system is maintained. However, it is noteworthy that this effect appears to mainly take place 1 year after the surgery, which indicates that it takes the ocular surface a notable time to recover from the effects of topical glaucoma medications and increased IOP.

The proteins increasing after the trabeculectomy are less well-known in connection to tear film and e.g. although MUCL1 has been identified in the tear film, its functions remain unclear. Lipid-binding apolipoproteins APOE and APOM have not been previously identified in tear fluid and it is possible that they originate from the epithelium cells or mucin layer, which can be included in the Schirmer strips. They can also be interacting with the lipid layer on the surface of the tear film due to their connections to lipid and cholesterol production and clearance. VPS4A is also connected to the lipid transport according to the STRING network. Although the precise effects of these proteins on the ocular surface are still unknown, high level of high-density lipoproteins (HDL) cholesterol ratio have been shown to reduce the likelihood of dry eye disease (Moss et al. 2000), while hyperlipidemia, i.e. increased low-density lipoprotein (LDL) and decreased HDL levels in blood, has been associated with an increased risk of glaucoma and increased IOP (Yilmaz et al. 2016, reviewed by Wang & Bao 2019). However, levels of lipid transporting proteins have not been previously examined from tear fluid in relation to glaucoma. Previous articles have discussed proteins, which remove lipids from the epithelial and mucin layers to prevent lipid contamination and help maintain tear film homeostasis thus making lipid transport a crucial part of functioning tear film (Setälä et al. 2010, Glasgow et al. 2010). Therefore, the identified proteins in our study, together with the results indicating an increased HDL particle function and lipid and cholesterol transport after the surgery could

mean that the previously administered topical glaucoma medications and/or increased IOP disrupted the normal lipid transport and HDL particle functions in the ocular surface. This could be then leading to tear film instability, which was eventually balanced after cessation of the topical treatment and a decrease of IOP.

In conclusion, both clinical signs as well as the proteomics results indicated that the trabeculectomy and resulting cessation of topical glaucoma medication were very beneficial to the ocular surface. Conjunctival grading scores reduced throughout the 1-year follow up, similar to decreased levels of pro-inflammatory proteins, while lipid transport-associated proteins were increased. It is worth noting that lipid transport and ROS-related functions' increase took place at the end time point, suggesting that the ocular surface recovery on protein level from irritation caused by topical treatment is a long process.

Acknowledgements

Personal financial interests:

A.V.: none

J.N.: none

F.G.: none

References

Almatlouh A, Bach-Holm D & Kessel L (2019): Steroids and nonsteroidal anti-inflammatory drugs in the postoperative regime after trabeculectomy - which provides the better outcome? A systematic review and meta-analysis. Acta Ophthalmol 97:146-157.

Breusegem C, Spielberg L, Van Ginderdeuren R et al. (2010): Preoperative nonsteroidal anti-inflammatory drug or steroid and outcomes after trabeculectomy: a randomized controlled trial. Ophthalmology 117:1324-1330.

Broadway DC, Grierson I, O'Brien C & Hitchings RA (1994): Adverse effects of topical antiglaucoma medication: II. The outcome of filtration surgery. Arch Ophthalmol 112:1446-1454.

Cairns JE (1968): Trabeculectomy: preliminary report of a new method. Am J Ophthalmol 66:673-679.

Dogru M, Kojima T, Simsek C & Tsubota K (2018): Potential role of oxidative stress in ocular surface inflammation and dry eye disease. Invest Ophthalmol Vis Sci 59:DES163-168.

Ferreira SM, Lerner SF, Brunzini R, Evelson PA & Llesuy SF (2004): Oxidative stress markers in aqueous humor of glaucoma patients. Am J Ophthalmol 137:62-69.

Flaxman SR, Bourne RRA, Resnikoff S et al. (2017): Vision Loss Expert Group of the Global Burden of Disease Study. Global causes of blindness and distance vision impairment 1990-2020: a systematic review and meta-analysis. Lancet Glob Health 5:1221-1234.

Gazzard G, Konstantakopoulou E, Garway-Heath D et al. (2019): LiGHT Trial Study Group. Selective laser trabeculoplasty versus eye drops for first-line treatment of ocular hypertension and glaucoma (LiGHT): a multicentre randomised controlled trial. Lancet 393:1505-1516.

Glasgow BJ, Gasymov OK, Abduragimov AR, Engle JJ & Casey RC (2010): Tear lipocalin captures exogenous lipid from abnormal corneal surfaces. Invest Ophthalmol Vis Sci 51:1981-1987.

Glaucoma. Current Care Guidelines (2014): Working group set up by the Finnish Medical Society Duodecim and the Finnish Glaucoma Society. Helsinki: The Finnish Medical Society Duodecim (referred 1st March 2020). Available online at: www.kaypahoito.fi.

Helin M, Rönkkö S, Puustjärvi T, Teräsvirta M, Ollikainen M & Uusitalo H (2011): Conjunctival inflammatory cells and their predictive role for deep sclerectomy in primary open-angle glaucoma and exfoliation glaucoma. J Glaucoma 20:172-178.

Helin-Toiviainen M, Rönkkö S, Puustjärvi T, Rekonen P, Ollikainen M & Uusitalo H (2015): Conjunctival matrix metalloproteinases and their inhibitors in glaucoma patients. Acta Ophthalmol 93:165-171.

Ighodaro OM & Akinloye OA (2018): First line defence antioxidants-superoxide dismutase (SOD), catalase (CAT) and glutathione peroxidase (GPX): Their fundamental role in the entire antioxidant defence grid. Alexandria J 54:287-293.

Jylhä A, Nättinen J, Aapola U, Mikhailova A, Nykter M, Zhou L, Beuerman R & Uusitalo H (2018): Comparison of iTRAQ and SWATH in a clinical study with multiple time points. Clin Proteom 15:24.

Landers J, Martin K, Sarkies N, Bourne R & Watson P (2012): A twenty-year follow-up study of trabeculectomy: risk factors and outcomes. Ophthalmology 119:694-702.

Lee RMH, Bouremel Y, Eames I, Brocchini S & Khaw PT (2019): Translating minimally invasive glaucoma surgery devices. Clin Transl Sci 13:14-25.

Leung YF & Pang CP (2002): EYE on bioinformatics: dissecting complex disease traits in silico. Appl Bioinformatics 1:69-80.

Li Z, Van Bergen T, Van de Veire S et al. (2009): Inhibition of vascular endothelial growth factor reduces scar formation after glaucoma filtration surgery. Invest Ophthalmol Vis Sci 50:5217-5225.

Liu X, Jann J, Xavier C & Wu H (2015): Glutaredoxin 1 (Grx1) protects human retinal pigment epithelial cells from oxidative damage by preventing AKT glutathionylation. Invest Ophthalmol Vis Sci 56:2821-2832.

Mansouri K, Medeiros FA & Weinreb RN (2013): Global rates of glaucoma surgery. Graefes Arch Clin Exp Ophthalmol 251:2609-2615.

Migdal C, Gregory W & Hitchings R (1994): Long-term functional outcome after early surgery compared with laser and medicine in open-angle glaucoma. Ophthalmology 101:1651-1657.

Moss SE, Klein R & Klein BE (2000): Prevalence of and risk factors for dry eye syndrome. Arch Ophthalmol 118:1264-1268.

Nordmann JP, Lepen C, Lilliu H & Berdeaux G (2003): Estimating the long-term visual field consequences of average daily intraocular pressure and variance. Clin Drug Investig 23:431-438.

Nättinen J, Jylhä A, Aapola U, Parkkari M, Mikhailova A, Beuerman R & Uusitalo H (2018): Patient stratification in clinical glaucoma trials using the individual tear proteome. Sci Rep 8:12038.

Nättinen J, Aapola U, Jylhä A, Vaajanen A & Uusitalo H (2020): Comparison of capillary and Schirmer strip tear fluid sampling methods using SWATH-MS proteomics approach. Transl Vis Sci Techn 9:16-.

Parkkari M, Taipale J & Uusitalo H (2019): Comparing glaucoma medications and general demographics in a sample of glaucoma patients treated in private practice with nationwide registry data in Finland. Acta Ophthalmol [Epub ahead of print].

Perumal N, Funke S, Pfeiffer N & Grus FH (2016): Proteomics analysis of human tears from aqueous-deficient and evaporative dry eye patients. Sci Rep 6:1-2.

Pieragostino D, Bucci S, Agnifili L et al. (2012): Differential protein expression in tears of patients with primary open angle and pseudoexfoliative glaucoma. Mol Biosys 8:1017-1028.

Roudkenar MH, Kuwahara Y, Baba T, Roushandeh AM, Ebishima S, Abe S, Ohkubo Y & Fukumoto M (2007): Oxidative stress induced lipocalin 2 gene expression: addressing its expression under the harmful conditions. J Radiat Res 48:39-44.

Setälä NL, Holopainen JM, Metso J et al. (2010): Interaction of phospholipid transfer
    protein with human tear fluid mucins. J Lipid Res 51:3126-3134.

Shah M (2019): Micro-invasive glaucoma surgery - an interventional glaucoma revolution.
    Eye Vis (Lond) 6:1-5.

Skuta GL and Parrish RK (1987): Wound healing in glaucoma filtering surgery. Surv
    Ophthalmol 32: 149-170.

Sun J, Wei X, Lu Y, Cui M, Li F, Lu J, Liu Y & Zhang X (2017): Glutaredoxin 1 (GRX1)
    inhibits oxidative stress and apoptosis of chondrocytes by regulating CREB/HO-1
    in osteoarthritis. Mol Immunol 90:211-218.

Szklarczyk D, Gable AL, Lyon D et al. (2019): STRING v11: protein-protein association
    networks with increased coverage, supporting functional discovery in genome-
    wide experimental datasets. Nucleic Acids Res 47:D607-613.

Tang W, Ma J, Gu R, Ding X, Lei B, Wang X, Zhuang H & Xu G (2018): Lipocalin 2
    suppresses ocular inflammation by inhibiting the activation of NF-κβ pathway in
    endotoxin-induced uveitis. Cell Physiol Biochem 46:375-388.

Uusitalo H, Chen E, Pfeiffer N et al. (2010): Switching from a preserved to a preservative-
    free prostaglandin preparation in topical glaucoma medication. Acta Ophthalmol
    88:329-336.

Uusitalo H, Egorov E, Kaarniranta K, Astakhov Y & Ropo A (2016): Benefits of switching
    from latanoprost to preservative-free tafluprost eye drops: a meta-analysis of two
    Phase IIIb clinical trials. Clin Ophthalmol 10:445.

Vandewalle E, Abegão Pinto L, Van Bergen T et al. (2014): Intracameral bevacizumab as an adjunct to trabeculectomy: a 1-year prospective, randomised study. Br J Ophthalmol 98:73-78.

Wang S & Bao X (2019): Hyperlipidemia, blood lipid level, and the risk of glaucoma: a meta-analysis. Invest Ophthalmol Vis Sci 60:1028-1043.

Wilkins M, Indar A & Wormald R (2005): Intraoperative mitomycin C for glaucoma surgery. Cochrane Db Syst Rev 4.

Wong TT, Zhou L, Li J et al. (2011): Proteomic profiling of inflammatory signaling molecules in the tears of patients on chronic glaucoma medication. Invest Ophth Vis Sci 52:7385-7391.

Yilmaz N, Coban DT, Bayindir A et al. (2016): Higher serum lipids and oxidative stress in patients with normal tension glaucoma, but not pseudoexfoliative glaucoma. Bosnian J Basic Med 16:21.

Zhang X, Vadoothker S, Munir WM & Saeedi O (2019): Ocular surface disease and glaucoma medications: a clinical approach. Eye Contact Lens 45:11-18.

Zhou L, Beuerman RW, Chan CM et al. (2009): Identification of tear fluid biomarkers in dry eye syndrome using iTRAQ quantitative proteomics. J Proteome Res 8:4889-4905.

FIGURE LEGENDS

Figure 1. Study outline describing pre- and postoperative medication duration (top) as well as clinical examination, medical information collection and tear fluid proteomics analysis (bottom) for patients during the visits.

Figure 2. A) Blinded[a] and B) unblinded[b] conjunctival grades and C) IOP (mmHg) values preoperatively (0) and in the months following the surgery (1, 3, 6 and 12 months after surgery). The values are reported as mean±SD. Conjunctival grading scores are on an ordinal scale (0-4). All postoperative time points had significantly decreased values in comparison to the preoperative values. D) Ocular surface images of a patient with a severe ocular surface irritation at the initial preoperative visit (0). Trabeculectomy was performed to the eye due to primary open-angle glaucoma, which had been treated topically for the past 14 years. The following images illustrate how the state of the conjunctiva improves 1, 3, 6 and 12 months after the surgery.

Figure 3. A selection of proteins with consistently changed expression levels after trabeculectomy. The y-axis expression levels (in $\log_2$-scale) indicate the change from preoperative levels (0, horizontal line). For most of the proteins displayed here, the difference to preoperative levels is consistent through the visits (x-axis). * = p-value < 0.05; ** = p-value < 0.01; *** = p-value < 0.001

Figure 4. Protein-protein networks of down- and upregulated proteins (A and B respectively) after a successful trabeculectomy. The downregulated proteins (43 out of 48) and upregulated proteins (17) were constructed into networks with STRING. The thickness of the networks edges (lines) indicates the strength of data support for a given protein connection. The color of the node indicates the proteins' connection to a given GO function (legend at the bottom).

Figure 5. Changes in biological functions 1, 3, 6 and 12 months (x-axis) after a successful trabeculectomy. Only non-disease-specific terms with an absolute Z-score > 2 and p-value < 0.05 in at least one time point are included. Biological functions (left, y-axis) are grouped into more general categories (right, y-axis) and the size of the balloon designates the p-value size (larger size indicates lower p-value). The colour of the balloon describes the direction of the change according to the z-score; blue indicates a decrease and red indicates an increase in the biological function after the surgery.

Patient's own medication

Chloramphenicol

Dexamethasone

| 0 | S | 1 | 3 | 6 | 12 |

Preoperative visit

Surgery

Postoperative visits (months after surgery)
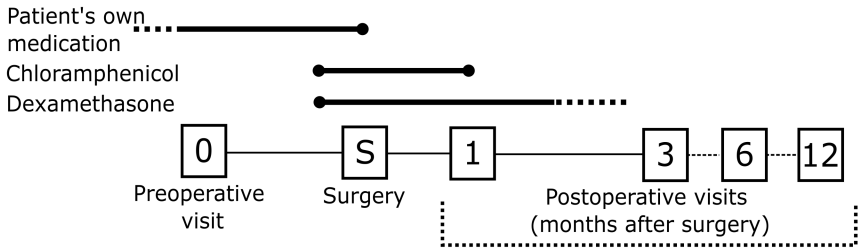
Clinical examination* including IOP, visual acuity, Schirmer's test and conjunctival reaction

👁 n = 57 ✓ ✓ ✓ ✓ ✓

Medical information of previous treatments/procedures, diagnosis etc.

📋 n = 57 ✓

Tear proteomics analysis

🩸 n = 33 ✓ ✓ ✓ ✓ ✓

*Visual fields (MD and VFI) were recorded only preoperatively and 1-year after the operation. Corneal pachymetry was performed only preoperatively.

A
Conjunctival grade[a] vs. Months from surgery

B
Conjunctival grade[b] vs. Months from surgery

C
IOP (mmHg) vs. Months from surgery

D
0 1 3 6 12

A

Immune effector process
Transport
Oxidation-reduction process
Secretion by cell
[Empty]

B

Immune effector process
Cellular component organization
Vesicle-mediated transport
Cholesterol transport
[Empty]
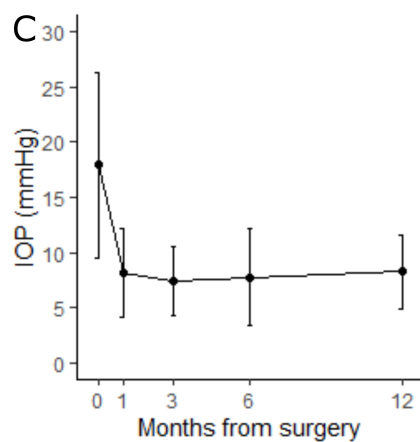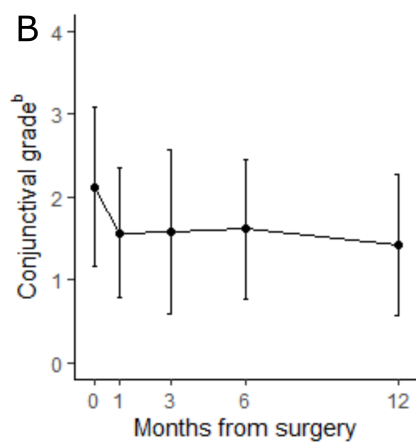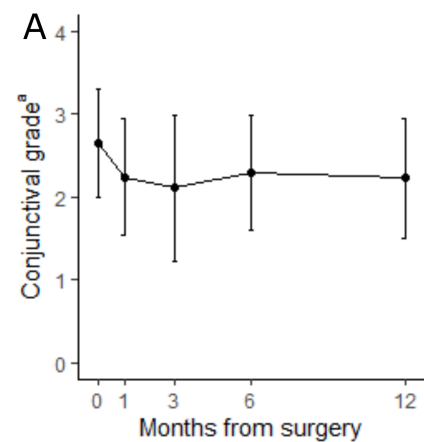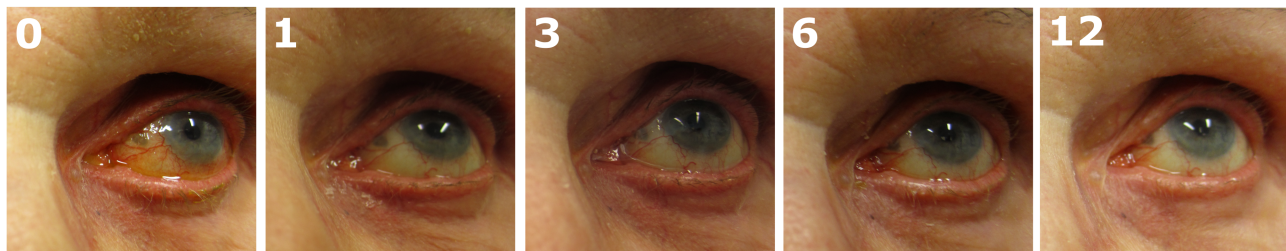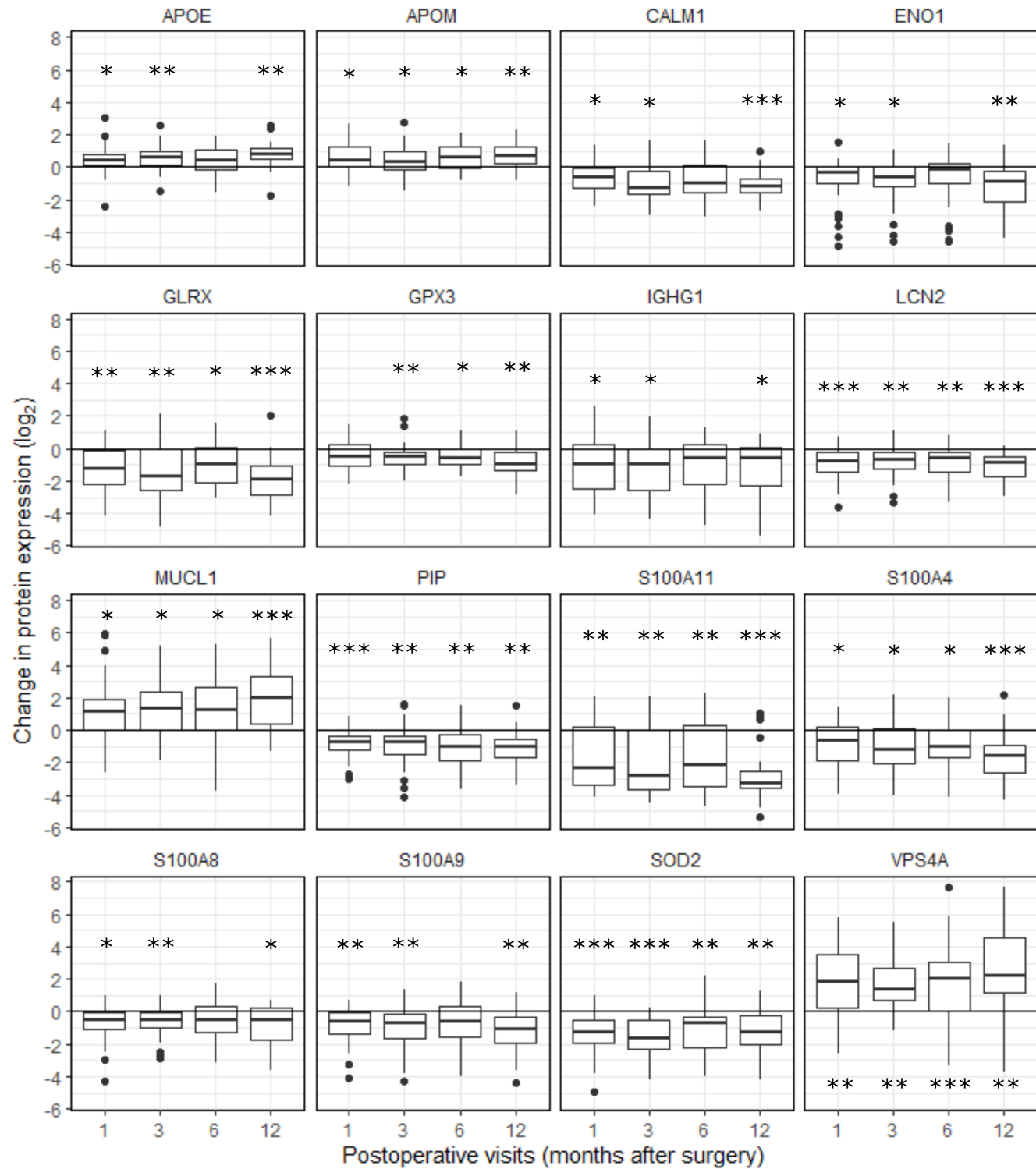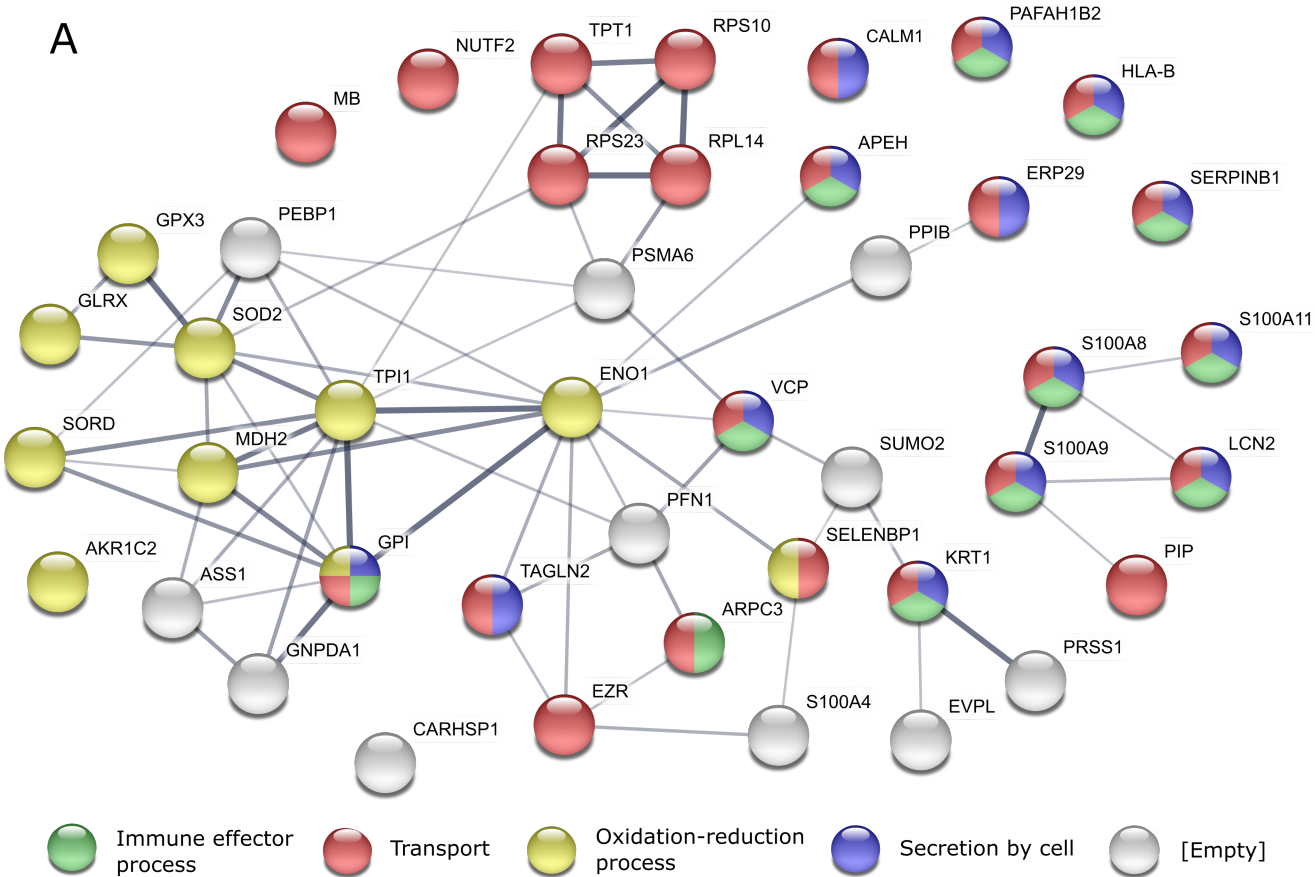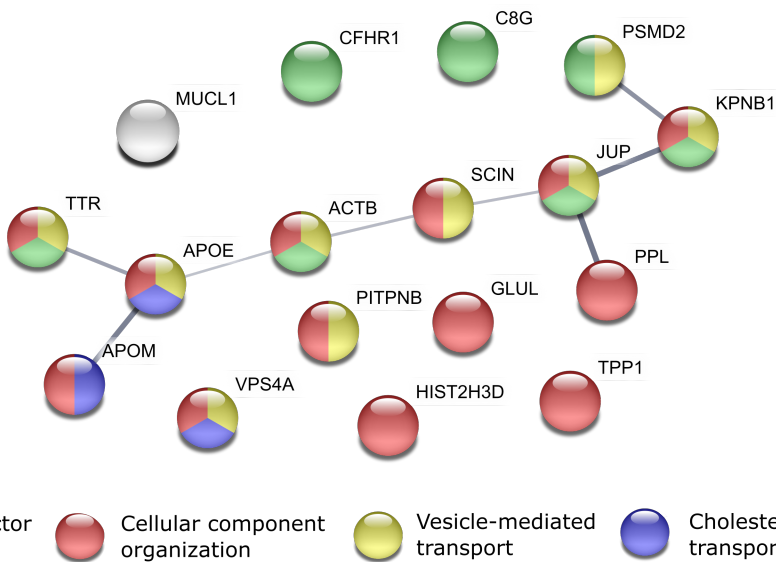
Supplementary Table S2

A list of proteins, which were significantly changed 1 year after the surgery

Uniprot	Full name	Symbol	Differen Median
P07477	Trypsin-1	PRSS1	-2,316
Q71DI3	Histone H3.2	HIST2H3A	1,872
P46926	Glucosamine-6-phosphate isomerase 1	GNPDA1	-1,796
P80188	Neutrophil gelatinase-associated lipocalin	LCN2	-0,858
P31949	Protein S100-A11	S100A11	-3,318
P01763	Ig heavy chain V-III region WEA	NA	-0,640
P62158	Calmodulin	CALM1	-1,198
Q9Y2V2	Calcium-regulated heat stable protein 1	CARHSP1	-1,558
P60900	Proteasome subunit alpha type-6	PSMA6	-1,267
P35754	Glutaredoxin-1	GLRX	-1,896
P07195	L-lactate dehydrogenase B chain	LDHB	-0,972
P61956	Small ubiquitin-related modifier 2	SUMO2	-0,659
P00966	Argininosuccinate synthase	ASS1	-1,003
P02766	Transthyretin	TTR	0,642
P06331	Ig heavy chain V-II region ARH-77	NA	-0,998
Q96DR8	Mucin-like protein 1	MUCL1	1,975
P61970	Nuclear transport factor 2	NUTF2	-0,719
P37802	Transgelin-2	TAGLN2	-1,147
P36952	Serpin B5	SERPINB5	-0,884
P26447	Protein S100-A4	S100A4	-1,571
P30086	Phosphatidylethanolamine-binding protein 1	PEBP1	-1,230
Q9Y6U3	Adseverin	SCIN	0,811
P14923	Junction plakoglobin	JUP	0,394
P23284	Peptidyl-prolyl cis-trans isomerase B	PPIB	-0,771
Q13200	26S proteasome non-ATPase regulatory subunit 2	PSMD2	0,774
P46783	40S ribosomal protein S10	RPS10	-1,338
P07737	Profilin-1	PFN1	-0,817
P53634	Dipeptidyl peptidase 1	CTSC	1,186
P06744	Glucose-6-phosphate isomerase	GPI	-0,493
P68402	Platelet-activating factor acetylhydrolase IB subunit beta	PAFAH1B2	-1,606
P12273	Prolactin-inducible protein	PIP	-1,007
P02649	Apolipoprotein E	APOE	0,799
O15145	Actin-related protein 2/3 complex subunit 3	ARPC3	-0,744
Q9UN37	Vacuolar protein sorting-associated protein 4A	VPS4A	2,226
P60174	Triosephosphate isomerase	TPI1	-0,726
P13693	Translationally-controlled tumor protein	TPT1	-0,749
O95445	Apolipoprotein M	APOM	0,647
P15311	Ezrin	EZR	-0,664
P06703	Protein S100-A6	S100A6	0,846
P04430	Ig kappa chain V-I region BAN	NA	-0,685
P06702	Protein S100-A9	S100A9	-1,131
P14550	Alcohol dehydrogenase [NADP(+)]	AKR1A1	-0,541
P30740	Leukocyte elastase inhibitor	SERPINB1	-1,218
P07360	Complement component C8 gamma chain	C8G	0,502
P50453	Serpin B9	SERPINB9	1,318

Q08257	Quinone oxidoreductase	CRYZ	-0,803
Q14974	Importin subunit beta-1	KPNB1	0,293
P13798	Acylamino-acid-releasing enzyme	APEH	-0,468
P06326	Ig heavy chain V-I region Mot	NA	-0,746
P06733	Alpha-enolase	ENO1	-0,875
Q9HC38	Glyoxalase domain-containing protein 4	GLOD4	-0,479
P61158	Actin-related protein 3	ACTR3	-0,607
Q96DA0	Zymogen granule protein 16 homolog B	ZG16B	-1,126
P40926	Malate dehydrogenase, mitochondrial	MDH2	-1,193
P01834	Ig kappa chain C region	IGKC	-0,706
O95834	Echinoderm microtubule-associated protein-like 2	EML2	-0,339
P01761	Ig heavy chain V-I region SIE	NA	0,992
P01833	Polymeric immunoglobulin receptor	PIGR	-0,675
Q9NZT1	Calmodulin-like protein 5	CALML5	-0,923
P15559	NAD(P)H dehydrogenase [quinone] 1	NQO1	-1,171
P04179	Superoxide dismutase [Mn], mitochondrial	SOD2	-1,272
O14773	Tripeptidyl-peptidase 1	TPP1	0,660
P49913	Cathelicidin antimicrobial peptide	CAMP	0,822
P05387	60S acidic ribosomal protein P2	RPLP2	-0,976
O43768	Alpha-endosulfine	ENSA	0,876
O75874	Isocitrate dehydrogenase [NADP] cytoplasmic	IDH1	-0,621
P80748	Ig lambda chain V-III region LOI	NA	-1,024
P22352	Glutathione peroxidase 3	GPX3	-1,002
Q6YHU6	REVERSED Thyroid adenoma-associated protein	THADA	1,034
P63104	14-3-3 protein zeta/delta	YWHAZ	-0,517
P01859	Ig gamma-2 chain C region	IGHG2	-0,473
P04632	Calpain small subunit 1	CAPNS1	-0,795
Q9P1F3	Costars family protein ABRACL	ABRACL	-0,865
P02144	Myoglobin	MB	-0,882
Q04760	Lactoylglutathione lyase	GLO1	-0,559
P01889	HLA class I histocompatibility antigen, B-7 alpha chain	HLA-B	-1,645
P20073	Annexin A7	ANXA7	-1,051
P00390	Glutathione reductase, mitochondrial	GSR	-0,503
P62266	40S ribosomal protein S23	RPS23	-1,632
P47895	Aldehyde dehydrogenase family 1 member A3	ALDH1A3	-0,465
P01719	Ig lambda chain V-V region DEL	NA	0,807
P06396	Gelsolin	GSN	-0,640
Q92817	Envoplakin	EVPL	-0,956
P61769	Beta-2-microglobulin	B2M	-0,382
P0CG05	Ig lambda-2 chain C regions	IGLC2	0,866
P52566	Rho GDP-dissociation inhibitor 2	ARHGDIB	-0,602
Q9NTK5	Obg-like ATPase 1	OLA1	-0,371
O43488	Aflatoxin B1 aldehyde reductase member 2	AKR7A2	-1,602
P68032	Actin, alpha cardiac muscle 1	ACTC1	0,648
Q15109	Advanced glycosylation end product-specific receptor	AGER	-0,748
P46459	Vesicle-fusing ATPase	NSF	0,418
P30040	Endoplasmic reticulum resident protein 29	ERP29	-0,829
P52895	Aldo-keto reductase family 1 member C2	AKR1C2	-0,643
O60888	Protein CutA	CUTA	-0,415
P61026	Ras-related protein Rab-10	RAB10	-0,774

P07384	Calpain-1 catalytic subunit	CAPN1	-0,638
P00734	Prothrombin	F2	0,654
B0FP48	Uroplakin-3b-like protein	UPK3BL	-0,519
P01624	Ig kappa chain V-III region POM	NA	0,337
P31944	Caspase-14	CASP14	0,358
Q9UHV9	Prefoldin subunit 2	PFDN2	1,502
P04264	Keratin, type II cytoskeletal 1	KRT1	-0,768
P04114	Apolipoprotein B-100	APOB	0,371
Q11201	CMP-N-acetylneuraminate-beta-galactosamide-alpha-2,3-sialyltransfera	ST3GAL1	0,450
Q9BPX5	Actin-related protein 2/3 complex subunit 5-like protein	ARPC5L	-0,636
Q53EL6	Programmed cell death protein 4	PDCD4	-0,597
P08779	Keratin, type I cytoskeletal 16	KRT16	0,384
O95994	Anterior gradient protein 2 homolog	AGR2	-0,826
P15104	Glutamine synthetase	GLUL	0,398
Q00796	Sorbitol dehydrogenase	SORD	-0,391
P08865	40S ribosomal protein SA	RPSA	-0,506
B9A064	Immunoglobulin lambda-like polypeptide 5	IGLL5	-0,800
P01611	Ig kappa chain V-I region Wes	NA	-0,697
Q96IY4	Carboxypeptidase B2	CPB2	0,458
P50914	60S ribosomal protein L14	RPL14	-0,533
P01857	Ig gamma-1 chain C region	IGHG1	-0,633
P16152	Carbonyl reductase [NADPH] 1	CBR1	-0,405
Q92743	Serine protease HTRA1	HTRA1	0,402
Q14914	Prostaglandin reductase 1	PTGR1	0,671
P05452	Tetranectin	CLEC3B	0,673
O43175	D-3-phosphoglycerate dehydrogenase	PHGDH	0,512
P26373	60S ribosomal protein L13	RPL13	-0,214
P00450	Ceruloplasmin	CP	-0,411
P00558	Phosphoglycerate kinase 1	PGK1	-0,456
P55072	Transitional endoplasmic reticulum ATPase	VCP	-0,235
P14555	Phospholipase A2, membrane associated	PLA2G2A	0,809
Q15847	Adipogenesis regulatory factor	ADIRF	-0,480
P27482	Calmodulin-like protein 3	CALML3	-0,924
O75828	Carbonyl reductase [NADPH] 3	CBR3	-0,983
Q9ULZ3	Apoptosis-associated speck-like protein containing a CARD	PYCARD	-0,686
P10155	60 kDa SS-A/Ro ribonucleoprotein	TROVE2	0,627
Q8NBJ4	Golgi membrane protein 1	GOLM1	0,458
P48444	Coatomer subunit delta	ARCN1	0,864
P62829	60S ribosomal protein L23	RPL23	-0,653
Q13228	Selenium-binding protein 1	SELENBP1	-0,552
P30044	Peroxiredoxin-5, mitochondrial	PRDX5	-0,410
P22392	Nucleoside diphosphate kinase B	NME2	-0,487
O43242	26S proteasome non-ATPase regulatory subunit 3	PSMD3	-0,696
P30838	Aldehyde dehydrogenase, dimeric NADP-preferring	ALDH3A1	-0,623
Q9UBC9	Small proline-rich protein 3	SPRR3	0,683
P27487	Dipeptidyl peptidase 4	DPP4	0,879
P62249	40S ribosomal protein S16	RPS16	0,485
P61020	Ras-related protein Rab-5B	RAB5B	0,755
P04406	Glyceraldehyde-3-phosphate dehydrogenase	GAPDH	-0,339
Q01813	ATP-dependent 6-phosphofructokinase, platelet type	PFKP	-0,630

P60709	Actin, cytoplasmic 1	ACTB	0,604
Q02487	Desmocollin-2	DSC2	0,678
O60437	Periplakin	PPL	0,226
P25789	Proteasome subunit alpha type-4	PSMA4	-0,619
P01040	Cystatin-A	CSTA	1,143
P01011	Alpha-1-antichymotrypsin	SERPINA3	-0,405
Q01518	Adenylyl cyclase-associated protein 1	CAP1	-0,267
P28799	Granulins	GRN	0,532
P15153	Ras-related C3 botulinum toxin substrate 2	RAC2	0,751
Q08623	Pseudouridine-5-phosphatase	HDHD1	1,190
P23528	Cofilin-1	CFL1	-0,349
P16401	Histone H1.5	HIST1H1B	0,529
Q14103	Heterogeneous nuclear ribonucleoprotein D0	HNRNPD	1,218
Q06323	Proteasome activator complex subunit 1	PSME1	-0,727
P12035	Keratin, type II cytoskeletal 3	KRT3	0,242
P04080	Cystatin-B	CSTB	-0,627
Q06210	Glutamine--fructose-6-phosphate aminotransferase [isomerizing] 1	GFPT1	0,285
O95741	Copine-6	CPNE6	-0,442
P28072	Proteasome subunit beta type-6	PSMB6	0,954
Q15631	Translin	TSN	0,551
P00352	Retinal dehydrogenase 1	ALDH1A1	-0,352
P07900	Heat shock protein HSP 90-alpha	HSP90AA1	-0,481
Q03591	Complement factor H-related protein 1	CFHR1	0,444
Q9BUT1	3-hydroxybutyrate dehydrogenase type 2	BDH2	0,644
Q14247	Src substrate cortactin	CTTN	1,043
P08603	Complement factor H	CFH	0,243
P13489	Ribonuclease inhibitor	RNH1	-0,500
P28066	Proteasome subunit alpha type-5	PSMA5	-0,438
Q8N335	Glycerol-3-phosphate dehydrogenase 1-like protein	GPD1L	-1,099
P19021	Peptidyl-glycine alpha-amidating monooxygenase	PAM	0,767
O95171	Sciellin	SCEL	0,812
Q96L46	Calpain small subunit 2	CAPNS2	-0,590
O95968	Secretoglobin family 1D member 1	SCGB1D1	-0,946
P05109	Protein S100-A8	S100A8	-0,553
P55327	Tumor protein D52	TPD52	0,641
P09871	Complement C1s subcomponent	C1S	0,539
Q8WXG9	G-protein coupled receptor 98	GPR98	0,545
P61353	60S ribosomal protein L27	RPL27	-0,680
Q8WUM4	Programmed cell death 6-interacting protein	PDCD6IP	-0,336
P03973	Antileukoproteinase	SLPI	0,677
P08185	Corticosteroid-binding globulin	SERPINA6	0,473
O75367	Core histone macro-H2A.1	H2AFY	0,544
Q86X76	Nitrilase homolog 1	NIT1	0,688
P68104	Elongation factor 1-alpha 1	EEF1A1	-0,414
P50995	Annexin A11	ANXA11	-0,219
P07996	Thrombospondin-1	THBS1	0,332
P02656	Apolipoprotein C-III	APOC3	0,340
P30685	HLA class I histocompatibility antigen, B-35 alpha chain	HLA-B	-0,723
Q8IZP2	Putative protein FAM10A4	ST13P4	-0,450
P04899	Guanine nucleotide-binding protein G(i) subunit alpha-2	GNAI2	0,501

Q13885	Tubulin beta-2A chain	TUBB2A	0,753
Q96KP4	Cytosolic non-specific dipeptidase	CNDP2	-0,364
P11216	Glycogen phosphorylase, brain form	PYGB	0,301
P19652	Alpha-1-acid glycoprotein 2	ORM2	-0,579
P01717	Ig lambda chain V-IV region Hil	NA	0,372
P21399	Cytoplasmic aconitate hydratase	ACO1	-0,852
P0CG06	Ig lambda-3 chain C regions	IGLC3	0,542
P62888	60S ribosomal protein L30	RPL30	-0,834
Q16204	Coiled-coil domain-containing protein 6	CCDC6	0,413
Q9NR45	Sialic acid synthase	NANS	-0,462
Q14764	Major vault protein	MVP	-0,522
P04066	Tissue alpha-L-fucosidase	FUCA1	-0,801
P13647	Keratin, type II cytoskeletal 5	KRT5	-1,105
P31946	14-3-3 protein beta/alpha	YWHAB	0,748
P20160	Azurocidin	AZU1	1,065
P05161	Ubiquitin-like protein ISG15	ISG15	0,563
Q16181	Septin-7	SEPT7	-0,368
P19013	Keratin, type II cytoskeletal 4	KRT4	-0,780
P10643	Complement component C7	C7	0,597
P01778	Ig heavy chain V-III region ZAP	NA	0,409
Q9UHD0	Interleukin-19	IL19	0,868
Q12792	Twinfilin-1	TWF1	-0,500

ce to baseline (log$_2$)		P-value	Adjusted p-value
Mean	SD		
-1,861	0,947	0,000	0,000
1,943	1,338	0,000	0,000
-1,880	1,224	0,000	0,000
-1,051	0,871	0,000	0,000
-2,855	1,657	0,000	0,000
-0,786	0,660	0,000	0,000
-1,160	0,851	0,000	0,000
-1,616	1,160	0,000	0,000
-1,352	1,086	0,000	0,000
-1,810	1,312	0,000	0,000
-0,968	0,840	0,000	0,000
-0,891	0,920	0,000	0,001
-0,929	0,850	0,000	0,001
0,646	0,568	0,000	0,001
-0,900	0,763	0,000	0,001
2,025	1,905	0,000	0,001
-0,756	0,681	0,000	0,001
-1,193	1,056	0,000	0,001
-0,942	0,842	0,000	0,001
-1,707	1,507	0,000	0,001
-1,044	1,035	0,000	0,001
0,833	0,765	0,000	0,001
0,419	0,423	0,000	0,001
-0,863	0,839	0,000	0,001
0,860	0,856	0,000	0,001
-1,210	1,136	0,000	0,001
-1,264	1,401	0,000	0,001
1,181	1,168	0,000	0,001
-0,596	0,612	0,000	0,001
-1,766	1,809	0,000	0,001
-1,127	1,201	0,000	0,001
0,823	0,884	0,000	0,001
-0,851	0,820	0,000	0,001
2,623	2,757	0,000	0,001
-0,819	0,974	0,000	0,001
-0,735	0,733	0,000	0,001
0,729	0,752	0,000	0,001
-0,638	0,716	0,000	0,001
1,193	1,337	0,000	0,001
-0,783	0,862	0,000	0,002
-1,264	1,387	0,000	0,002
-0,767	0,884	0,000	0,002
-0,987	1,004	0,000	0,002
0,533	0,590	0,000	0,002
1,301	1,333	0,000	0,002

-1,118	1,377	0,000	0,002
0,479	0,555	0,000	0,002
-0,494	0,514	0,000	0,002
-0,814	0,894	0,000	0,002
-1,178	1,517	0,000	0,002
-0,484	0,533	0,000	0,002
-0,598	0,658	0,000	0,002
-1,329	1,580	0,000	0,002
-1,157	1,291	0,000	0,002
-0,993	1,214	0,000	0,003
-0,374	0,418	0,000	0,003
0,919	1,029	0,000	0,003
-0,915	1,174	0,000	0,003
-0,903	1,057	0,000	0,003
-1,017	1,119	0,000	0,003
-1,192	1,375	0,000	0,003
0,567	0,646	0,000	0,003
0,950	1,191	0,000	0,003
-0,880	1,051	0,000	0,003
0,943	1,158	0,000	0,003
-0,589	0,739	0,000	0,004
-1,193	1,524	0,000	0,004
-0,861	1,009	0,000	0,004
1,175	1,612	0,000	0,004
-0,581	0,746	0,000	0,004
-0,749	1,215	0,000	0,004
-0,643	0,790	0,000	0,004
-0,828	1,013	0,000	0,004
-0,824	0,973	0,000	0,004
-0,573	0,745	0,000	0,005
-1,349	1,639	0,000	0,005
-0,868	1,007	0,001	0,006
-0,509	0,702	0,001	0,006
-1,284	1,580	0,001	0,006
-0,431	0,554	0,001	0,007
0,899	1,267	0,001	0,007
-0,675	0,861	0,001	0,008
-0,790	1,099	0,001	0,008
-0,610	0,968	0,001	0,009
0,969	1,268	0,001	0,009
-0,515	0,697	0,001	0,009
-0,529	0,732	0,001	0,009
-1,121	1,413	0,001	0,009
0,916	1,263	0,001	0,009
-0,769	0,992	0,001	0,009
0,386	0,514	0,001	0,010
-0,853	1,197	0,001	0,010
-0,831	1,103	0,001	0,010
-0,659	0,945	0,001	0,011
-0,821	1,144	0,001	0,011

-0,427	0,690	0,001	0,011
0,386	0,783	0,001	0,011
-0,546	0,733	0,001	0,011
0,614	0,855	0,001	0,011
0,639	0,877	0,001	0,012
1,313	1,827	0,001	0,012
-0,735	1,013	0,002	0,013
0,470	0,821	0,002	0,013
0,658	0,867	0,002	0,013
-0,759	1,025	0,002	0,013
-0,501	0,676	0,002	0,015
0,341	0,525	0,002	0,015
-0,804	1,160	0,002	0,015
0,360	0,553	0,002	0,015
-0,454	0,661	0,002	0,015
-0,532	0,812	0,002	0,015
-0,948	1,337	0,002	0,015
-0,710	0,976	0,002	0,015
0,585	0,985	0,002	0,015
-0,514	0,748	0,002	0,015
-1,280	1,660	0,002	0,016
-0,564	0,940	0,002	0,016
0,480	0,736	0,002	0,016
0,745	1,071	0,002	0,016
0,909	1,384	0,002	0,016
0,449	0,649	0,002	0,017
-0,719	1,308	0,002	0,017
-0,565	0,870	0,003	0,018
-0,845	1,251	0,003	0,018
-0,260	0,400	0,003	0,018
0,825	1,229	0,003	0,018
-0,735	1,156	0,003	0,018
-0,848	1,358	0,003	0,018
-0,789	1,209	0,003	0,018
-0,704	1,076	0,003	0,018
0,575	0,812	0,003	0,018
0,388	0,566	0,003	0,019
0,853	1,305	0,003	0,019
-0,697	1,057	0,003	0,019
-0,658	1,145	0,003	0,020
-0,589	0,972	0,003	0,020
-0,556	0,811	0,003	0,020
-0,655	1,078	0,003	0,020
-0,686	1,057	0,004	0,022
0,681	1,024	0,004	0,022
0,932	1,411	0,004	0,022
0,657	0,994	0,004	0,022
0,630	1,020	0,004	0,022
-0,496	0,806	0,004	0,023
-0,558	0,899	0,004	0,023

0,665	1,024	0,004	0,023
0,705	1,108	0,004	0,023
0,335	0,529	0,004	0,025
-0,541	0,902	0,004	0,025
1,356	2,203	0,004	0,025
-0,618	0,936	0,005	0,026
-0,324	0,614	0,005	0,026
0,471	0,743	0,005	0,026
0,798	1,491	0,005	0,026
0,834	1,318	0,005	0,026
-0,433	0,733	0,005	0,028
0,632	0,948	0,005	0,028
1,285	2,034	0,005	0,028
-0,556	0,902	0,006	0,030
0,338	0,528	0,006	0,030
-0,666	1,018	0,006	0,030
0,293	0,491	0,006	0,030
-0,526	1,014	0,006	0,030
0,994	1,576	0,006	0,030
0,658	1,108	0,006	0,030
-1,020	1,558	0,006	0,031
-0,441	0,832	0,006	0,031
0,437	0,718	0,006	0,031
0,605	1,030	0,006	0,031
0,954	1,636	0,006	0,031
0,361	0,667	0,007	0,033
-0,486	0,789	0,007	0,033
-0,345	0,600	0,007	0,033
-0,795	1,284	0,007	0,033
0,770	1,356	0,007	0,033
0,687	1,237	0,007	0,033
-0,595	1,097	0,007	0,033
-0,729	1,340	0,007	0,035
-0,794	1,194	0,007	0,035
0,501	0,861	0,007	0,035
0,502	0,860	0,007	0,035
0,706	1,193	0,007	0,035
-0,652	1,094	0,007	0,035
-0,313	0,541	0,008	0,037
0,575	0,962	0,008	0,037
0,529	0,963	0,008	0,037
0,503	0,859	0,008	0,037
0,613	1,058	0,008	0,037
-0,433	0,857	0,009	0,038
-0,296	0,566	0,009	0,038
0,437	0,793	0,009	0,038
0,398	1,002	0,009	0,038
-0,710	1,223	0,009	0,038
-0,453	0,785	0,009	0,038
0,399	0,990	0,009	0,038

0,595	1,618	0,009	0,038
-0,383	0,729	0,009	0,040
0,219	0,428	0,009	0,040
-0,609	1,086	0,009	0,040
0,480	0,845	0,009	0,040
-0,542	0,970	0,009	0,040
0,584	1,098	0,009	0,040
-0,617	1,124	0,009	0,040
0,300	0,642	0,010	0,043
-0,507	0,904	0,010	0,043
-0,448	0,876	0,010	0,043
-0,789	1,295	0,010	0,043
-0,777	1,508	0,011	0,045
0,675	1,243	0,011	0,045
0,806	1,382	0,011	0,045
0,641	1,142	0,011	0,045
-0,837	1,527	0,011	0,045
-0,871	1,517	0,012	0,048
0,604	1,014	0,012	0,048
0,440	0,868	0,012	0,048
0,958	1,693	0,012	0,048
-0,461	0,829	0,012	0,048

Supplementary Table S3
Proteins with altered expression level after the surgery in at least 3 time point comparisons. Statistically sign

Uniprot	Full name	Symbol	Differe P vs 1
P31949	Protein S100-A11	S100A11	-2,353
P07477	Trypsin-1	PRSS1	-1,633
P60900	Proteasome subunit alpha type-6	PSMA6	-1,358
P04179	Superoxide dismutase [Mn], mitochondrial	SOD2	-1,306
P35754	Glutaredoxin-1	GLRX	-1,296
P01889	HLA class I histocompatibility antigen, B-7 alpha chain	HLA-B	-1,016
P46783	40S ribosomal protein S10	RPS10	-0,914
P46926	Glucosamine-6-phosphate isomerase 1	GNPDA1	-0,810
P00966	Argininosuccinate synthase	ASS1	-0,797
P80188	Neutrophil gelatinase-associated lipocalin	LCN2	-0,768
P12273	Prolactin-inducible protein	PIP	-0,759
P30740	Leukocyte elastase inhibitor	SERPINB1	-0,705
P37802	Transgelin-2	TAGLN2	-0,690
Q9Y2V2	Calcium-regulated heat stable protein 1	CARHSP1	-0,647
P26447	Protein S100-A4	S100A4	-0,625
P30040	Endoplasmic reticulum resident protein 29	ERP29	-0,514
P06326	Ig heavy chain V-I region Mot	NA	-0,510
P52895	Aldo-keto reductase family 1 member C2	AKR1C2	-0,447
P13693	Translationally-controlled tumor protein	TPT1	-0,433
P07737	Profilin-1	PFN1	-0,398
P13798	Acylamino-acid-releasing enzyme	APEH	-0,237
Q14974	Importin subunit beta-1	KPNB1	0,346
Q03591	Complement factor H-related protein 1	CFHR1	0,385
O95445	Apolipoprotein M	APOM	0,421
O14773	Tripeptidyl-peptidase 1	TPP1	0,486
Q9Y6U3	Adseverin	SCIN	0,679
Q13200	26S proteasome non-ATPase regulatory subunit 2	PSMD2	0,778
Q71DI3	Histone H3.2	HIST2H3A	1,051
Q96DR8	Mucin-like protein 1	MUCL1	1,163
Q9UN37	Vacuolar protein sorting-associated protein 4A	VPS4A	1,856
P14923	Junction plakoglobin	JUP	0,402
P02144	Myoglobin	MB	-0,648
P06331	Ig heavy chain V-II region ARH-77	NA	-0,535
P60709	Actin, cytoplasmic 1	ACTB	0,437
P01763	Ig heavy chain V-III region WEA	NA	-0,492
Q92817	Envoplakin	EVPL	-0,746
P15104	Glutamine synthetase	GLUL	0,596
Q13228	Selenium-binding protein 1	SELENBP1	-0,459
P06702	Protein S100-A9	S100A9	-0,661
P55072	Transitional endoplasmic reticulum ATPase	VCP	-0,252
P48739	Phosphatidylinositol transfer protein beta isoform	PITPNB	0,486
P68402	Platelet-activating factor acetylhydrolase IB subunit beta	PAFAH1B2	-1,037
P05109	Protein S100-A8	S100A8	-0,508
P15311	Ezrin	EZR	-0,279
P62158	Calmodulin	CALM1	-0,595

Q00796	Sorbitol dehydrogenase	SORD	-0,345
P02649	Apolipoprotein E	APOE	0,388
P06744	Glucose-6-phosphate isomerase	GPI	-0,319
P30086	Phosphatidylethanolamine-binding protein 1	PEBP1	-0,528
P06733	Alpha-enolase	ENO1	-0,340
P61970	Nuclear transport factor 2	NUTF2	-0,349
P01857	Ig gamma-1 chain C region	IGHG1	-1,006
P07360	Complement component C8 gamma chain	C8G	0,490
P50914	60S ribosomal protein L14	RPL14	-0,619
P23284	Peptidyl-prolyl cis-trans isomerase B	PPIB	-0,477
P61956	Small ubiquitin-related modifier 2	SUMO2	-0,453
P62266	40S ribosomal protein S23	RPS23	-1,232
P40926	Malate dehydrogenase, mitochondrial	MDH2	-0,661
P04264	Keratin, type II cytoskeletal 1	KRT1	-0,499
O60437	Periplakin	PPL	0,337
P22352	Glutathione peroxidase 3	GPX3	-0,519
P02766	Transthyretin	TTR	0,292
P30685	HLA class I histocompatibility antigen, B-35 alpha chain	HLA-B	-0,726
P60174	Triosephosphate isomerase	TPI1	-0,181
O15145	Actin-related protein 2/3 complex subunit 3	ARPC3	-0,332

| ence to baseline (log$_2$ median) | | | Adjusted p-value | | | |
P vs 3	P vs 6	P vs 12	P vs 1	P vs 3	P vs 6	P vs 12
-2,801	-2,194	-3,318	0,004	0,004	0,007	0,000
-1,808	-2,102	-2,316	0,000	0,001	0,002	0,000
-1,319	-1,164	-1,267	0,000	0,003	0,002	0,000
-1,674	-0,676	-1,272	0,000	0,000	0,007	0,003
-1,729	-0,984	-1,896	0,002	0,005	0,018	0,000
-1,225	-1,009	-1,645	0,006	0,005	0,025	0,005
-0,726	-0,885	-1,338	0,022	0,014	0,041	0,001
-1,702	-1,442	-1,796	0,012	0,026	0,009	0,000
-0,955	-0,514	-1,003	0,000	0,003	0,024	0,001
-0,708	-0,615	-0,858	0,001	0,005	0,002	0,000
-0,709	-1,028	-1,007	0,000	0,007	0,005	0,001
-0,717	-0,535	-1,218	0,001	0,003	0,041	0,002
-0,905	-0,608	-1,147	0,006	0,005	0,020	0,001
-1,163	-1,089	-1,558	0,003	0,011	0,027	0,000
-1,188	-1,044	-1,571	0,032	0,022	0,035	0,001
-0,646	-0,542	-0,829	0,017	0,022	0,027	0,010
-0,424	-0,914	-0,746	0,001	0,023	0,009	0,002
-0,635	-0,668	-0,643	0,037	0,033	0,044	0,010
-0,419	-0,660	-0,749	0,011	0,015	0,011	0,001
-0,677	-0,527	-0,817	0,021	0,021	0,041	0,001
-0,496	-0,287	-0,468	0,037	0,010	0,040	0,002
0,372	0,452	0,293	0,019	0,026	0,003	0,002
0,729	0,459	0,444	0,039	0,000	0,041	0,031
0,340	0,572	0,647	0,020	0,047	0,019	0,001
0,504	0,548	0,660	0,021	0,022	0,019	0,003
0,723	0,726	0,811	0,000	0,000	0,002	0,001
0,655	0,811	0,774	0,000	0,004	0,007	0,001
1,137	1,937	1,872	0,019	0,014	0,006	0,000
1,323	1,213	1,975	0,020	0,015	0,032	0,001
1,314	1,984	2,226	0,002	0,001	0,007	0,001
0,284	0,262	0,394	0,000	0,059	0,037	0,001
-0,609	-1,009	-0,882	0,019	0,071	0,019	0,004
-0,679	-0,893	-0,998	0,013	0,056	0,006	0,001
0,430	0,547	0,604	0,049	0,087	0,005	0,023
-0,374	-0,585	-0,640	0,018	0,059	0,004	0,000
-0,601	-1,037	-0,956	0,018	0,177	0,003	0,008
0,416	0,495	0,398	0,000	0,005	0,053	0,015
-0,622	-0,371	-0,552	0,000	0,016	0,105	0,020
-0,732	-0,617	-1,131	0,002	0,004	0,092	0,002
-0,324	-0,091	-0,235	0,006	0,007	0,251	0,018
0,242	0,368	0,411	0,007	0,014	0,003	0,090
-1,377	-0,793	-1,606	0,012	0,011	0,148	0,001
-0,566	-0,529	-0,553	0,017	0,008	0,134	0,035
-0,608	-0,256	-0,664	0,017	0,013	0,157	0,001
-1,299	-1,017	-1,198	0,018	0,010	0,061	0,000

-0,313	-0,252	-0,391	0,019	0,043	0,173	0,015
0,613	0,369	0,799	0,021	0,005	0,116	0,001
-0,339	-0,264	-0,493	0,023	0,020	0,100	0,001
-0,889	-0,418	-1,230	0,023	0,034	0,241	0,001
-0,625	-0,154	-0,875	0,032	0,014	0,250	0,002
-0,569	-0,352	-0,719	0,032	0,005	0,073	0,001
-1,014	-0,590	-0,633	0,032	0,022	0,074	0,016
0,518	0,328	0,502	0,037	0,022	0,110	0,002
-0,891	-0,159	-0,533	0,042	0,015	0,591	0,015
-0,860	-0,385	-0,771	0,045	0,039	0,074	0,001
-0,390	-0,231	-0,659	0,049	0,045	0,053	0,001
-1,315	-1,258	-1,632	0,050	0,015	0,010	0,006
-1,358	-1,461	-1,193	0,056	0,020	0,005	0,002
-0,503	-0,876	-0,768	0,128	0,041	0,003	0,013
0,263	0,352	0,226	0,056	0,022	0,007	0,025
-0,523	-0,631	-1,002	0,057	0,008	0,034	0,004
0,357	0,435	0,642	0,098	0,020	0,003	0,001
-0,593	-0,518	-0,723	0,098	0,036	0,048	0,038
-0,524	-0,264	-0,726	0,118	0,026	0,034	0,001
-0,534	-0,458	-0,744	0,208	0,043	0,040	0,001